

SUPPLEMENTARY MATERIAL

Polymorphs of Neutral Red, a Redox-Mediating Phenazine in Biological Systems

Mackenzie Labine-Romain,^a Sabrina Beckmann,^a Mohan Bhadbhade,^b Saroj Bhattacharyya,^b
Michael Manefield,^a Christopher E. Marjo,^{*b} Anne M. Rich.^b

^aSchool of Chemical Engineering, University of New South Wales, Kensington, NSW 2052, Australia

^bMark Wainwright Analytical Centre, Room G61, Chemical Sciences Building (F10), University of New South Wales, Kensington, NSW 2052, Australia

*Corresponding author. Tel.: +612 9385 4693; fax: +612 9385 4663.

E-mail address: c.marjo@unsw.edu.au

Table S1: Minimal mineral media used for crystallisation of Form II of neutral red.

Component	Concentration (g L ⁻¹)
KBr	0.1
CaCl ₂ .2H ₂ O	0.2
MgCl ₂ .6H ₂ O	2.6
NaCl	20
NH ₄ Cl	0.25
KH ₂ PO ₄	0.2
KCl	0.5

Also contains 1x trace elements and vitamin solutions described in Tables S2 and S3.

Table S2: Vitamin solution (1000x)

Component	Concentration (mg L⁻¹)
Biotin	2.0
Folic acid	2.0
Pyridoxine-HCl	10.0
Thiamine-HCl . 2H ₂ O	5.0
Riboflavin	5.0
Nicotinic acid	5.0
D-Ca-pantothenate	5.0
Vit B ₁₂	0.1
4-aminobenzoic acid	5.0
Lipoic acid	5.0

Table S3: Trace element solution (1000x)

Component	Concentration (g L⁻¹)
Nitriloacetic acid	1.50
MgSO ₄ .7H ₂ O	3.00
MnCl ₂ .4H ₂ O	0.50
NaCl	1.00
FeSO ₄ .7H ₂ O	0.10
CoCl ₂ .6H ₂ O	0.18
CaCl ₂ .2H ₂ O	0.10
ZnSO ₄ .7H ₂ O	0.18
CuSO ₄ .5H ₂ O	0.01
H ₃ BO ₃	0.01
Na ₂ MoO ₄ .2H ₂ O	0.01
NiCl ₂ .6H ₂ O	0.03
Na ₂ SeO ₃ .5H ₂ O	0.0003
Na ₂ WO ₄ .2H ₂ O	0.004

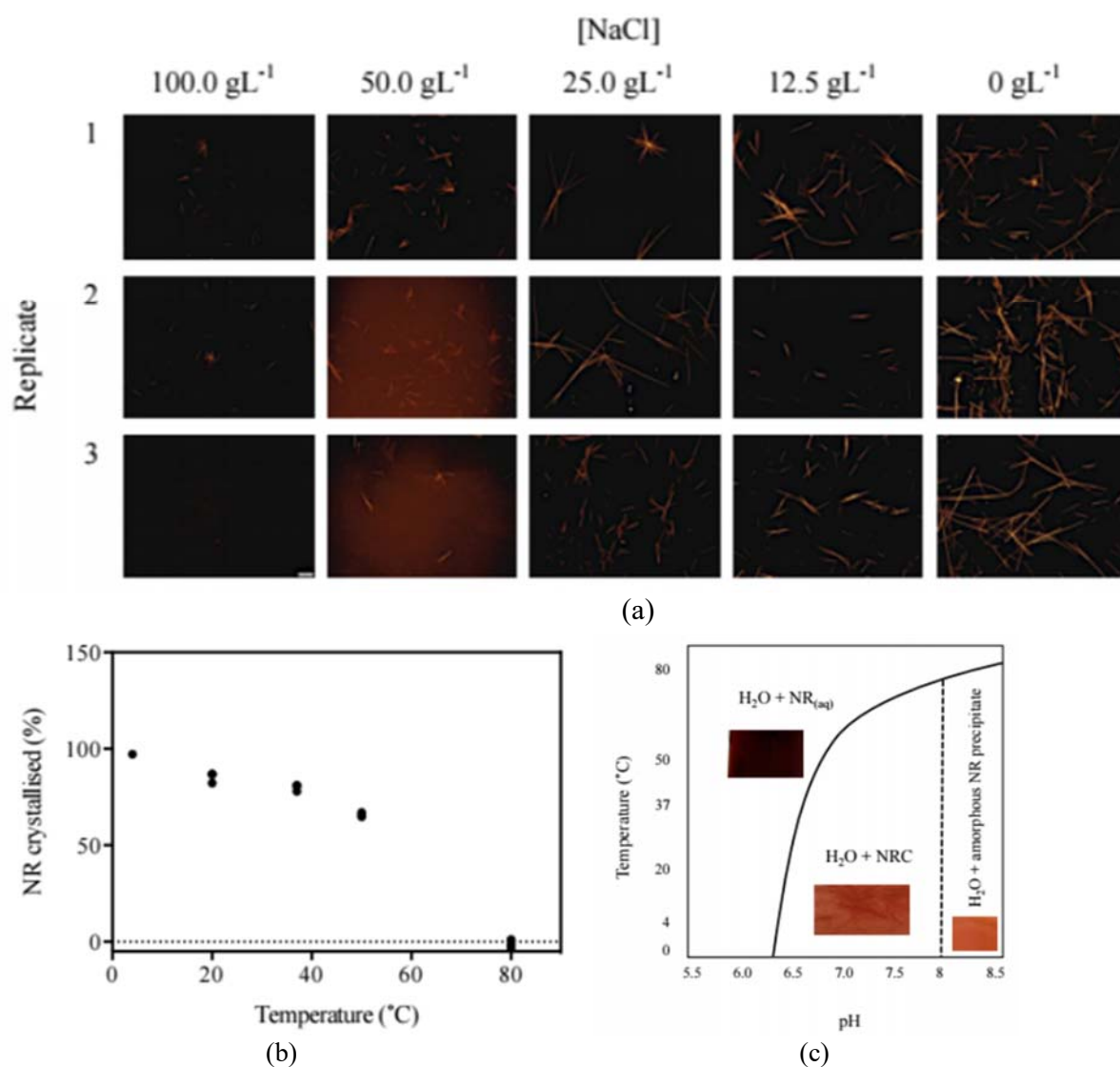


Figure S1: Crystallisation experiments on 250 μM aqueous solutions of neutral red. (a) Effect of changing salinity levels on crystallisation after 9 days, imaged using fluorescence microscopy at 10x. High salt levels produced a majority of brown amorphous precipitate, and the highest yield of microcrystals was obtained at zero salinity. (b) Wt% yield of crystalline neutral red obtained at different temperatures, as determined by spectrophotometry of solutions after 9 days. (c) Phase diagram of neutral red where the region below the solid curve indicates the where precipitation will occur. The region to the left of the broken line is where crystalline materials forms, and the region to the right of the broken line represents where the precipitate is an amorphous solid.

Table S4: Intermolecular contact areas from Hirshfeld analysis of the asymmetric unit for Forms I and II.

Internal atom...External atom	Form I %	Form II %
C...C	5.4	5.3
C...H	6.6	6.7
C...N	2.1	2.1
C...O	0	0
N...C	2.1	2
N...N	0	0
N...H	2.5	2.4
N...O	0	0
H...C	6.1	6.2
H...N	2.3	2.3
H...H	55.6	55
H...O	7.9	8.1
O...C	0	0
O...N	0	0
O...H	9.4	9.8
O...O	0	0
Total	100	99.9

Table S5: Peak positions of the significant peaks from the Raman and infrared spectroscopy of Forms I and II

	Form I (cm ⁻¹)	Form II (cm ⁻¹)
Raman	198	199*
	294*	301
	453*	454
	477	475*
	501*	501
	639	640
	767	767
	1215	1215
	1232	1232
	1312	1311
	1365	1365
	1378	1378
	1417	1417
	1489	1489
	1562	1562
FTIR	808	808
	1008	1009
	1189	1190
	1309	1309
	1437	1437
	1484	1486
	1503	1503
	1604	1606
	3227	3223
	3338	3332

* Denotes a higher intensity peak in one form relative to the other (only observed in the Raman).

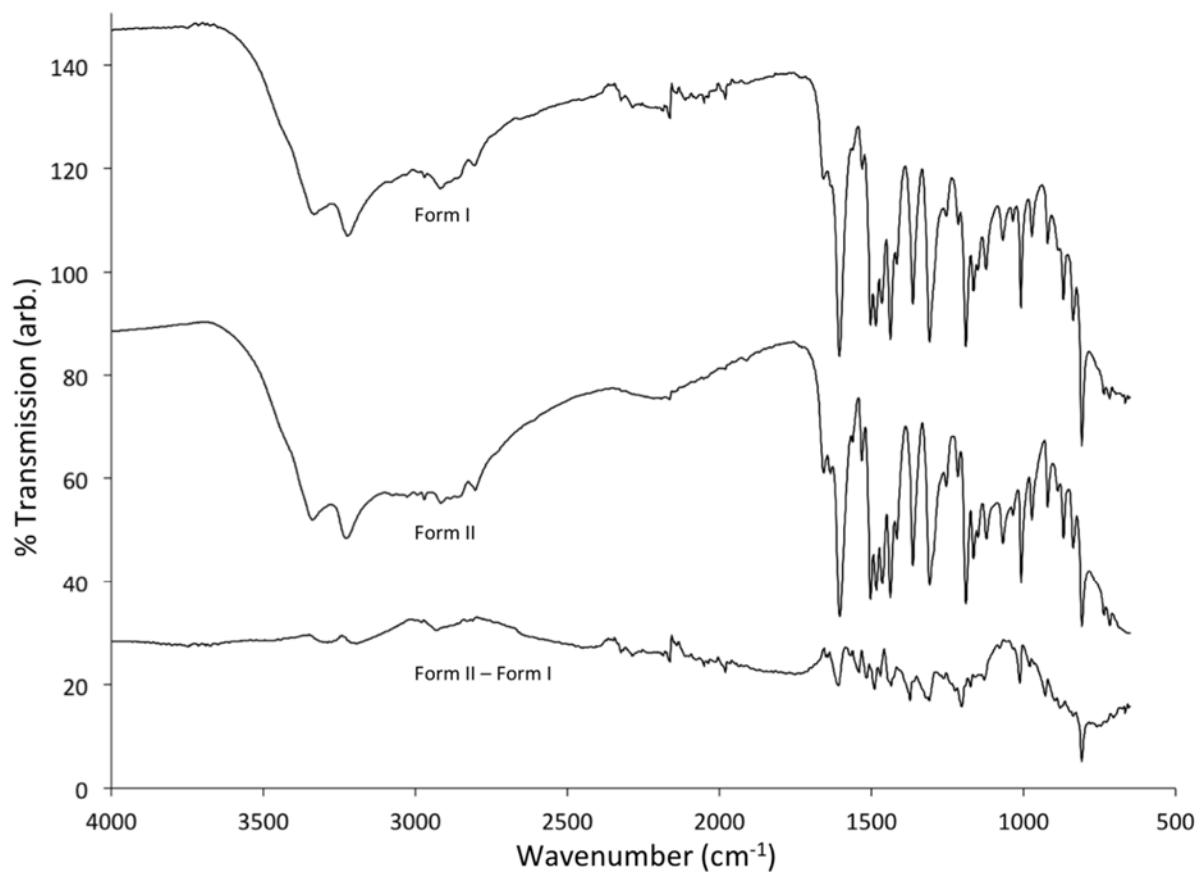


Figure S2: Percent transmission ATR-FTIR spectra of Forms I and II, scaled for comparison, showing difference spectrum.

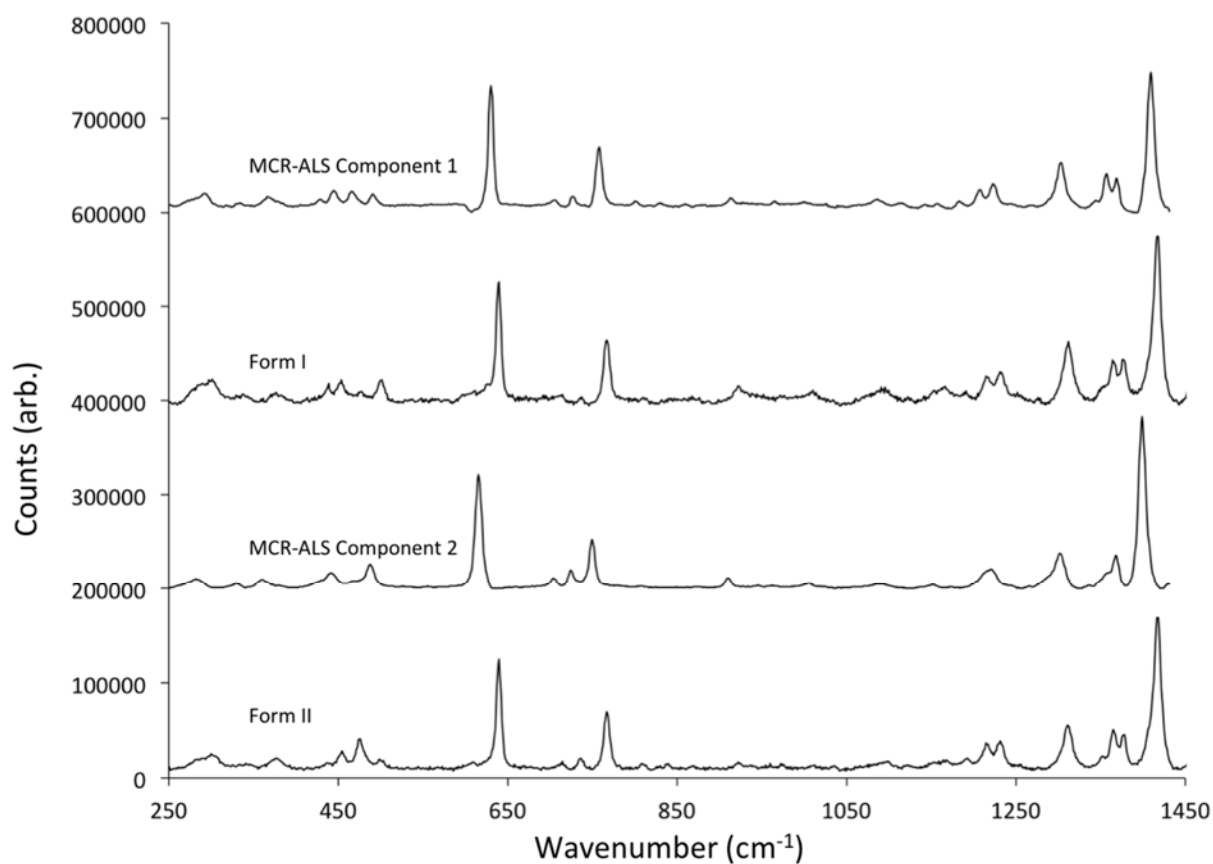


Figure S3: Comparison of standard Raman spectra and components extracted from imaging data using MCR-ALS. A close match is observed between Form I and Component 1, however significant changes in peak position are observed between Form II and Component 2 that may be due to dehydration or light induced chemical changes during imaging.